Received: 16 June 2021 | Revised: 11 November 2021 | Accepted: 14 December 2021

DOI: 10.1002/gj.4377

RESEARCH ARTICLE

WILEY

Geomorphic evaluation of landslides along the Teesta river valley, Sikkim Himalaya, India

Vikram Gupta[1] | **Neha Chauhan**[1] | **Ivanna Penna**[2] | **Reginald Hermanns**[2] | **John Dehls**[2] | **Aniruddha Sengupta**[3] | **Rajinder K. Bhasin**[4]

[1]Wadia Institute of Himalayan Geology, Dehradun, India

[2]Geological Survey of Norway, Trondheim, Norway

[3]Indian Institute of Technology, Kharagpur, India

[4]Norwegian Geotechnical Institute, Oslo, Norway

Correspondence
Vikram Gupta, Wadia Institute of Himalayan Geology, Dehradun, India.
Email: vgupta_wihg@yahoo.com

Funding information
Research Council of Norway; Ministry of Earth Sciences

Handling Editor: A.K. Singh

Landslides are a common and widespread phenomena in tectonically active mountains, impacting on landscape development, and lanslides pose a serious threat to the lives and properties when these interfere with humans and their associated infrastructure. However, the spatial distribution of these landslides is controlled by various geological and geomorphological parameters, including the neotectonic activity and the climatic pattern of the area. In the present study, various geomorphic parameters such as longitudinal and topographic swath profile, valley floor width to valley height ratio, channel steepness index, and stream length gradient index, along with the rainfall pattern of the Teesta river valley, Sikkim Himalaya, were correlated with the spatial distribution of landslides in the area. It has been concluded that landslides in the Higher Himalaya, north of the Main Central Thrust behind the orographic barrier, owe their origin mainly to the higher tectonic activity, and adjacent to the Main Central Thrust in the front of the orographic barrier to both tectonic activity and the higher rainfall. The distribution of landslides in the Lesser Himalaya is dominantly controlled by lithology and is mainly triggered by the rainfall.

KEYWORDS
geomorphic parameters, Himalaya, landslides, neotectonic, Sikkim

1 | INTRODUCTION

In the tectonically active mountains, landslides are widespread phenomena, impacting on landscape development (Allen, Cox, & Owens, 2011; Gerrard, 1994; Hewitt, 1988, 2002, 2006; Hovius, Stark, & Allen, 1997; Shroder & Bishop, 1998). Landslides transfer material from slopes to valley bottoms contributing to mountain erosion and are often conditioned by tectonics, climate, and anthropogenic activities (Agliardi, Crosta, Frattini, & Malusà, 2013; Hermanns, Niedermann, Garcia, Gomez, & Strecker, 2001; Korup, Densmore, & Schlunegger, 2010; Kumar, Gupta, & Sundriyal, 2019; Larsen & Montgomery, 2012; I. M. Penna, Hermanns, Niedermann, & Folguera, 2011; D. N. Petley et al., 2007; Sanchez et al., 2010; Tandon, Gupta, & Venkateshwarlu, 2021; Trauth, Alonso, Haselton, Hermanns, & Strecker, 2000). There is heterogeneous distribution of landslides around the globe with Asia representing the dominant geographical area (Froude & Petley, 2018). Around 15% of the Indian landmass is prone to different kinds of landslides, and these are mainly concentrated in the Himalayan terrain (BMTPC, 2003). These landslides pose a serious threat to lives and properties when these interfere with humans and their associated infrastructure. A rough estimate of the monetary loss is of the order of ~20 million USD per annum at the 2011 prices for the country as a whole which is ~30% of the total damage by landslides in the entire world (MHA, Govt. of India, 2011).

Lithology and structural conditions have a key role on the development of landslides in the Himalaya (Dortch et al., 2009; Jamir, Gupta, Thong, & Kumar, 2020). However, the frequency and magnitudes of landslides and the related mass movement activities have increased manifold during recent years in the Himalayan terrain. These are related to both natural and anthropogenic factors. The natural factors are mainly the increased incidences of extreme rainfall events, as well as the concentrated rainfall, particularly during the monsoon season (Gupta, Tandon, Venkateshwarlu, Bhasin, & Kaynia, 2017), whereas the anthropogenic factors are manifold, including change of slope geometry mainly related to construction, mining, and hill cutting. It is worth mentioning that landslides in the Himalaya do not distribute randomly, and are constrained to well-known landslide hot-spot zones (Nadim, Kjekstad, Peduzzi, Herold, & Jaedicke, 2006; D. Petley, 2012). In general, these are confined in the proximity of the weak zones marked by the thrusts and faults, as the rocks are highly weathered and shattered in these zones (Ghosh & Carranza, 2010; Kumar et al., 2019; Tandon et al., 2021). However, in the zones of glacial retreat and permafrost degradation, there is also higher possibility of slope instability mainly because of the degraded rock mass resulting from weathering, freeze, and thaw, and permafrost degradation (Krautblatter, Funk, & Günzel, 2013).

Sikkim Himalaya is known for the occurrences of numerous disastrous landslides (Anbalagan, Kumar, Lakshmanan, Parida, & Neethu, 2015; Anbarasu, Sengupta, Gupta, & Sharma, 2010; R. K. Bhasin et al., 2002; Mehrotra, Sarkar, Kanungo, & Mahadevaiah, 1996; I. Penna et al., 2021; Sengupta, Gupta, & Anbarasu, 2010; Sharma, Anbarasu, Gupta, & Sengupta, 2010). Despite the fact that these are triggered especially during the monsoon season or during or following earthquakes (R. Bhasin et al., 2020: Gupta, Mahajan, & Thakur, 2015; Mahajan, Gupta, & Thakur, 2012; Martha, Govindharaj, & Kumar, 2015; Morken, Hermanns, Penna, Dehls, & Bhasin, 2020; Singh & Singh, 2016; Weidinger & Korup, 2009), their spatial distribution points to local conditions controlling their location. By carrying out a systematic analysis along the Teesta river valley, our work aims to determine the main conditioning factors for the occurrence of landslides observed between Lachen and Rangpo (Figure 1).

2 | GENERAL SETTING

The study area is located in the northern part of Sikkim Himalaya. It comprises a ~95 km long stretch of the Teesta river valley between Lachen (27°43′00″N; 88°33′36″E) in the north and Rangpo (27°10′28″N; 88°31′17″E) in the south (Figure 1). The main tributaries of the Teesta River are Lachen Chhu and Lachung Chhu which join one another at Chungthang village. Lachen village is located at an altitude of ~2,700 m above sea level (asl) along the Lachen Chhu, whereas Rangpo is located at an altitude of ~300 m asl along the River Teesta.

Outcrops in the study area belong to the Lesser Himalaya and the Higher Himalaya (Figure 1). The main rock types constituting the Lesser Himalaya are phyllite, schist, and quartzite which can be grouped into the Gorubathan Formation of the Daling Group. These lesser Himalayan rocks are thrusted over by the rocks of the Higher Himalaya along a major shear zone called the Main Central Thrust (MCT). A sheet of 1–3 km thick contemporaneous deformed intrusive Lingste Granite Gneiss is present all along the MCT. The main rock types constituting the Higher Himalaya are schist and gneisses which are differentiated into the Chungthang Formation and the Darjeeling banded gneisses or Kanchanjunga augen gneisses (Acharyya, 1980; Saha, 2013). The greater part of the study area in the Higher Himalaya is occupied by the rocks of the Chungthang Formation which constitutes pelitic schists and gneisses.

Valley floor elevation ranges between <300 m asl near Rangpo and ~2,700 m asl near Lachen, whereas mountain top is about 700 m asl near Rangpo and ~4,700 m asl near Lachen. The valley slopes, in general, are steep (60°–75°) to very steep (>75°). The tributary Lachen Chhu joins the tributary Lachung Chhu at Chungthang to form the Teesta River, which flows from north to south till Shipgyer, and changes its course from Shipgyer and flows towards the south-west till Mangan, and further downstream until Rangpo. The general direction of the flow of the river is towards the south and SSW with fluctuation at places. Some of the geomorphic features present in the area are alluvial fans, terraces, flood plains, deep dissected valleys, and glacial and periglacial deposits. In general, U-shaped valleys dominate at higher elevations, particularly in the vicinity of Lachen, whereas V-shaped valleys formed by fluvial processes dominate at the lower elevations, near Rangpo. The areas in the vicinity of the towns of Mangan and Chungthang exhibit glacio-fluvial environment.

The area is seismically active and lies in the immediate eastern vicinity of the 1934 Great Bihar Nepal earthquake rupture zone. Earthquakes in this region are broadly associated with strain accumulation associated with the northward tectonic movement of the Indian Plate and its subsequent abrupt release. In the past, numerous earthquakes have been recorded in the area and its surroundings. Some of the noteworthy earthquakes in the region and its surroundings are summarized in Table 1.

The entire area of Sikkim lies in Zone IV of the Seismic Zonation Map of India (BIS, 2002) which is the second highest seismic zone. The seismic Zone IV is broadly associated with seismic intensity VIII on the Modified Mercalli Intensity (MMI) Scale.

3 | METHODOLOGY

3.1 | Landslide inventory

The inventory of all the active landslides was prepared using Pleiades 1A tri-stereo images (2018) having a resolution of 50 cm, LANDSAT 8 images (2016–2018) having a resolution of 15 m, and the satellite images for the years 2016, 2017, 2018, and 2019 on the Google Earth platform. Extensive fieldwork in the area was carried out to update and validate the inventory of landslides. These landslides were classified as either debris slide or rockfall on the basis of the type of the process involved.

3.2 | Longitudinal and topographic swath profile along the river

In the present study, the longitudinal profile and the 4 km wide topographic swath profile of the Teesta river with the river as midline were generated using the ALOS PALSAR DEM having 12.5 m resolution. The mean and maximum swath profiles were calculated along the trunk stream.

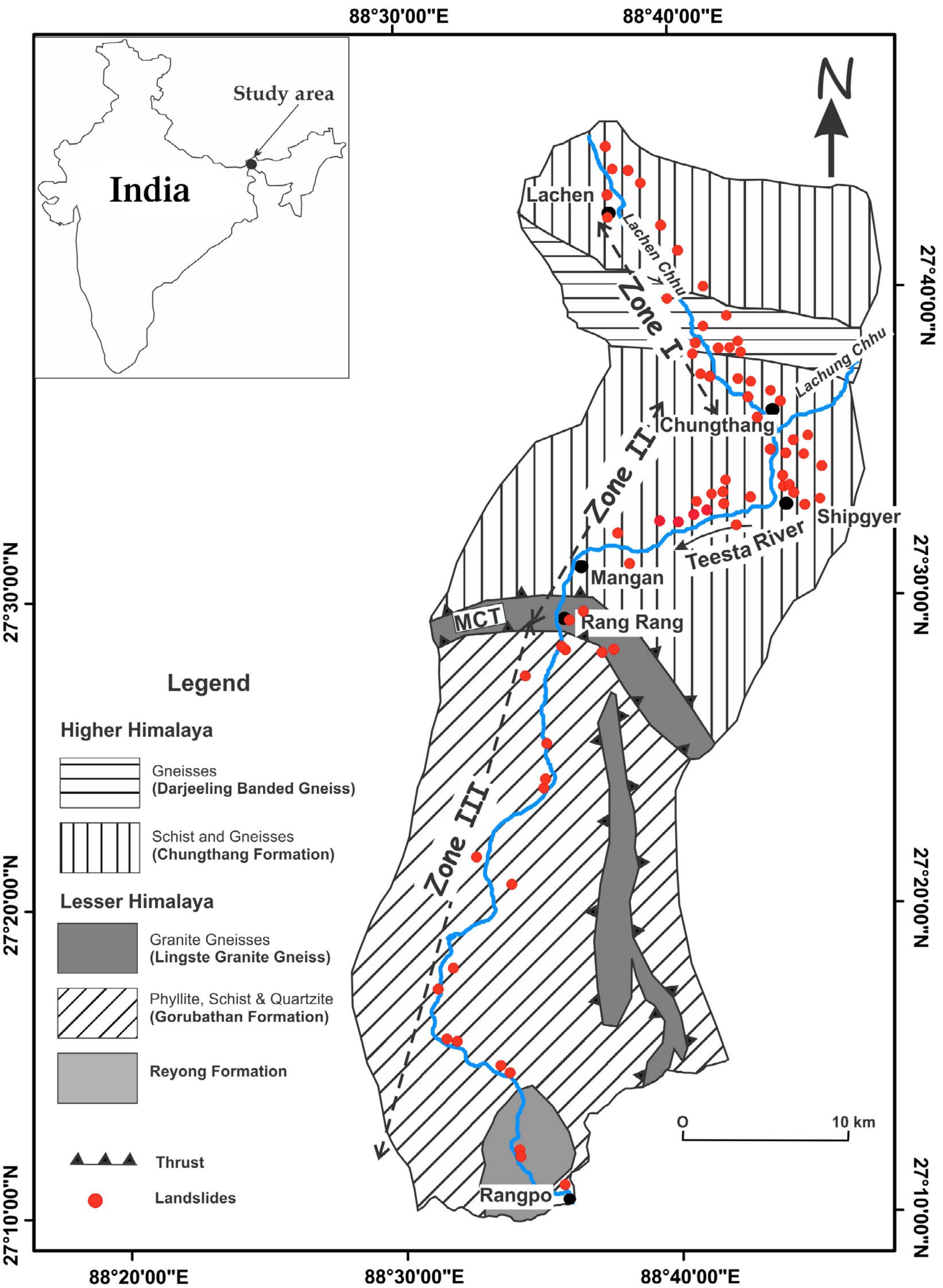

FIGURE 1 Location map of the study area indicating the geological set up. Three geomorphic zones along with the spatial distribution of landslides are also represented

3.3 | Morphotectonic indices

3.3.1 | Valley floor width to valley height ratio (V_f)

Valley floor width to valley height ratio (V_f), developed by Bull and McFadden (1977), allows differentiating between broad floored open valley and V-shaped deep narrow valley (Bull & McFadden, 1977; Keller & Pinter, 1996). It is represented by the following equation:

$$V_f = \frac{2V_{fw}}{[(E_{ld} - E_{sc}) + (E_{rd} - E_{sc})]},$$

Sl. No.	Earthquake	Date	Magnitude
1.	Cachar Earthquake	January 10, 1869	7.5
2.	Shillong Plateau Earthquake	June 12, 1897	8.0–8.7
3.	Dhubri Earthquake	July 2, 1930	7.1
4.	Bihar–Nepal Border Earthquake	January 15, 1934	7.5–8.4
5.	Arunachal Pradesh–China Border Earthquake	August 15, 1950	8.4–8.7
6.	Earthquake near Gangtok	November 19, 1980	6.1
7.	Nepal–India Border Earthquake	August 21, 1988	6.4
8.	Sikkim Earthquake	February 14, 2006	5.7
9.	Bhutan Earthquake	September 21, 2009	6.2
10.	Sikkim Earthquake	September 18, 2011	6.9
11	Gorkha Earthquake	April 25, 2015	7.8

TABLE 1 Table indicating the occurrence of earthquakes in the study area and its surroundings

where V_{fw} is the width of the valley floor, E_{ld} and E_{rd} are the elevations of the left and right valley divides, respectively, and E_{sc} is the elevation of the valley floor.

Low values of V_f (<1) correspond to V-shaped valleys, while high values (V_f > 1) reflect broad floored U-shaped valleys.

Using as input data the ALOS PALASR DEM, we have computed the V_f ratio for 316 cross sections distributed at regular interval of 300 m. To smoothen the peaks, the running average of four consecutive values was obtained.

3.3.2 | Channel steepness index (Ks)

Channel steepness index (Ks) is a measure of stream-channel gradient normalized to the drainage area (Wobus et al., 2006). It is described using stream power law function, which is derived from slope-area regression and has been calculated. It is given by the following equation:

$$S = K_s A^{-\theta},$$

where S represents the local channel slope, A represents the upstream drainage area, and K_s and θ represent the channel steepness and concavity indices.

K_s for the study area has been extracted at regular interval of 300 m along the Teesta river channel.

3.3.3 | Stream length gradient (SL) index

Stream length gradient (SL) index is a quantitative measure of gradient change along a river and is calculated by normalizing the river channel against the longest regional drainage (Hack, 1973; Keller & Pinter, 1996).

$$\mathrm{SL} = (\Delta H/\Delta L) \times L,$$

where ΔH is the difference of elevation of the reach, ΔL is the length of the reach, and L is the total channel length from the midpoint of the reach of interest upstream to the highest point on the channel.

4 | RESULTS

4.1 | Landslide distribution

An inventory of 71 active landslides having length > 20 m have been built along the Teesta River (Figure 1). An individual landslide covers an area ranging between ~600 and 700,000 m^2, with length varying between 25 and 1,200 m. The dimensional characteristics of each landslide are presented in Table 2. Most of these landslides are located in the vicinity of Mangan town near the MCT and further upstream.

4.2 | Morphotectonic proxies

It has been observed that the general longitudinal profile of the river is concave upward with average channel gradient of ~25 m/km. On the basis of channel gradient, the area has been divided into three zones (Figure 2), and the characteristic features of each zone are described in Table 3 and are summarized in the following.

4.2.1 | Zone I—Lachen to Chungthang

Zone I located between Lachen and Chungthang exhibits a channel gradient of the Teesta River of the order of ~50 m/km. This zone is ~22 km in length along the course of the river and lies in the Higher Himalaya. In general, the steepness index in this zone is high and ranges between 103 and 661, whereas the valley floor width to valley height ratio ranges between 0.014 and 0.114. The stream length gradient (SL) index for this zone is 1,110 (Figure 2). There are 26 landslides in this zone; thus, there is an average of ~1.18 landslides per km along the River Lachen Chhu.

This zone is located in the rain shadow zone, and thus, it receives less precipitation as compared to the other zones as evidenced by the Tropical Rainfall Measuring Mission (TRMM) rainfall data (Figure 2).

TABLE 2 The dimensional characteristics of each landslides in the three geomorphic zones

	Zone I			Zone II			Zone III		
Sr. no	Length of landslide (m)	Width of landslide (m)	Surface area (m^2)	Length of landslide (m)	Width of landslide (m)	Surface area (m^2)	Length of landslide (m)	Width of landslide (m)	Surface area (m^2)
1	363	142	51,546	204	27	5,508	127	60	7,620
2	988	130	128,440	227	61	13,847	37	32	1,184
3	166	149	24,734	282	132	37,224	201	89	17,889
4	122	85	10,370	51	24	1,224	42	17	714
5	285	36	10,260	196	82	16,072	55	38	2,090
6	192	62	11,904	230	70	16,100	135	190	25,650
7	113	46	5,198	101	43	4,343	235	122	28,670
8	315	60	18,900	104	24	2,496	212	177	37,524
9	369	241	88,929	109	60	6,540	216	50	10,800
10	183	80	14,640	317	62	19,654	240	55	13,200
11	135	54	7,290	299	72	21,528	74	85	6,290
12	280	53	14,840	591	57	33,687	88	29	2,552
13	25	25	625	112	17	1,904	57	33	1,881
14	51	37	1,887	234	36	8,424	218	112	24,416
15	65	23	1,495	176	20	3,520	1,140	234	266,760
16	287	155	44,485	293	65	19,045	1,200	558	669,600
17	106	65	6,890	195	85	16,575	144	61	8,784
18	57	28	1,596	141	63	8,883	205	81	16,605
19	198	59	11,682	488	38	18,544			
20	278	79	21,962	423	85	35,955			
21	512	211	108,032	595	63	37,485			
22	164	36	5,904	1,138	200	227,600			
23	370	238	88,060	187	279	52,173			
24	156	30	4,680	302	177	53,454			
25	136	72	9,792	525	238	124,950			
26	142	45	6,390	207	43	8,901			
27				184	66	12,144			

4.2.2 | Zone II—Chungthang to Rangrang

Zone II, located between Chungthang and Rangrang, exhibits a channel gradient of the Teesta River of the order of ~37 m/km. The zone is located to the immediate north of the Main Central Thrust (MCT). This zone is ~23 km in length and also lies in the Higher Himalaya. The steepness index in this zone varies between 84 and 678. This zone exhibits the highest value of steepness index (678) and the stream length gradient index (1640). The valley floor width to valley height ratio ranges between 0.110 and 0.023 (Figure 2). There are 27 landslides in this zone; thus, there is an average of ~1.17 landslides per km along the River Teesta.

This zone is located to the immediate front of the orographic barrier; thus, this zone is characterized by higher amount of rainfall as compared to rainfall in Zone I (Figure 2). Some of the major landslides such as Rangrang, Mantan, Lanta Khola, and Mangan landslides (Figure 3a–d) that are posing a threat to the inhabitants are located in this zone. Besides, there are many small-scale landslides in this zone that causes frequent damages particularly to the North Sikkim highway and to the habitation of the Mangan township.

4.2.3 | Zone III—Rangrang to Rangpo

Zone III, located between Rangrang and Rangpo, exhibits a gentle channel gradient of the Teesta River of the order of ~12 m/km. It is ~50 km in length along the course of the river and is located in the Lesser Himalaya. This zone exhibits lowest steepness index (52) and the highest valley floor width to valley height ratio (0.369), and also the lowest stream length gradient index (855). The V_f ratio in the area varies between 0.023 and 0.369 (Figure 2). There are 18 landslides in this zone; thus, there is an average of ~0.36 landslides per km along the River Teesta in this zone.

Furthermore, this zone experiences the highest annual rainfall as compared to the Zone I and Zone II (Figure 2).

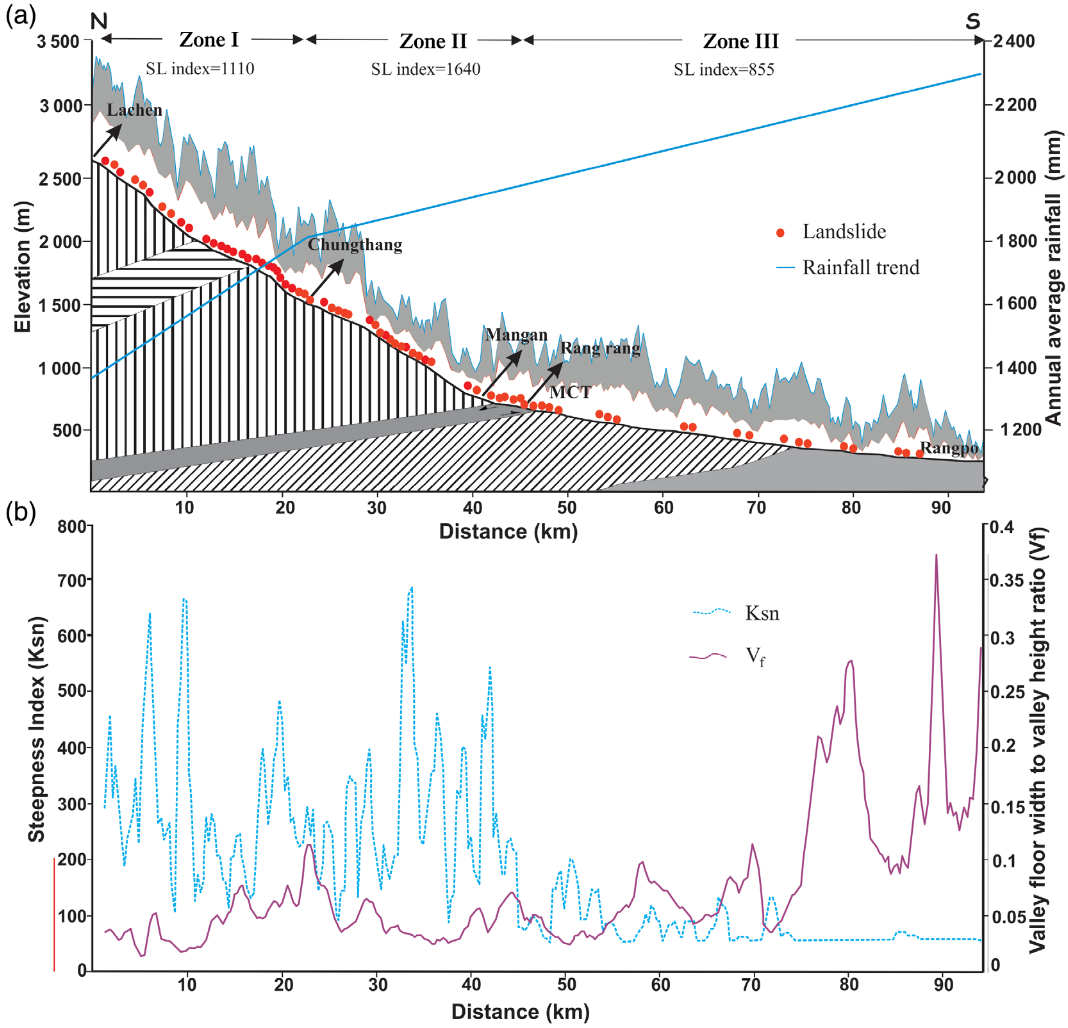

FIGURE 2 (a) Longitudinal profile of the Teesta River in a stretch between Lachen and Rangpo. The swath profile, the rainfall trend, the variations of stream length gradient index, and the distribution of landslides in the three geomorphic zones are also presented. (b) The variation in channel steepness index and the valley floor width to valley height ratio between Lachen and Rangpo

TABLE 3 The characteristic features of each of the three geomorphic zones in the area between Lachen and Rangpo in the study area

Parameters	Zone I	Zone II	Zone III
Average channel gradient	50 m/km	37 m /km	12 m/km
Number of landslides	26	27	18
Average area of each landslide	26,944 m^2	29,468 m^2	40,794 m^2
Steepness Index	103–661	84–678	52–202
Valley floor width to valley height ratio (V_f)	0.014–0.114	0.110–0.023	0.023–0.369
Stream length gradient index	1,110	1,640	855

In general, the V_f values are higher in the Lesser Himalaya as compared to the Higher Himalaya. The highest V_f value is observed near Rangpo in the Lesser Himalaya (Zone III). The lowest value is observed near Lachen in the Higher Himalaya (Zone I). Furthermore, Chungthang and Mangan exhibit relatively higher V_f values in the Higher Himalaya possibly due to the confluence of the tributaries. Furthermore, the values of K_s in general are higher in the Higher Himalaya (Zones I and II) as compared to the Lesser Himalaya (Zone III). There are also certain peaks of higher K_s value in Zone I and Zone II that generally coincide with the lithocontacts. The comparatively higher steepness index and stream length gradient index and lower valley floor width to valley height ratio in Zone I and Zone II indicate higher tectonic activity in these zones as compared to Zone III. This has further been corroborated with the higher values of stream length gradient (SL) index in Zone I and Zone II than in Zone III (Figure 2).

FIGURE 3 Some of the disastrous landslides between Mangan and Rangrang: (a) Rangrang landslide, (b) Mantan landslide, (c) Lanta Khola landslide, and (d) the landslide near Mangan township

5 | DISCUSSION

The spatial distribution of active landslides along the Teesta river valley in the Sikkim Himalaya, between Lachen and Rangpo, has been analysed, and in the following sections, we discuss the potential role of tectonic activity on the occurrence of the landslides.

Numerous studies indicate that various geomorphic indices are good proxies to determine the inherent tectonic activity in the region, which in turn affect the distribution of erosion potential and the development of landslides (Bull, 2009; Jamir et al., 2020; Kumar et al., 2019). In situ topographic stresses, resulting from interaction between tectonic stress and topography, also have considerable influence on rock deformation and play a vital role in weakening the rock mass and inducing landslides (G. K. Li & Moon, 2021; Panthi & Nilsen, 2006). In the present area of study, Zone I exhibiting the higher steepness index and the lower valley floor width to valley height ratio indicates higher tectonic activity. In this sector of the Teesta watershed, the higher tectonic activity has strongly influenced the development of slopes and is evidenced by the presence of steep and very steep valley slopes (Figure 4a), deep narrow gorges, and high topographic relief (Figure 4b), favouring the development of landslides. An example of this is the Yumthang rock avalanche involving ca. 12 millions of cubic meters of material developed on a valley slope of ~70° (I. Penna et al., 2021), similar to what has also been documented in the Higher Himalaya from other parts of the north-western Himalaya (Jamir et al., 2020; Kumar et al., 2019).

Zone II lies in the immediate vicinity of the MCT and also exhibits the highest steepness index, stream length gradient index, and lower valley floor width to valley height ratio. Thus, the tectonic activities in this zone are also high. This has been evidenced in the form of development of steep valley slopes, observed in the Teesta river valley and its tributaries. There is thus higher propensity of development of landslides in both the zones, and it is for this reason that there are higher chances of formation of the landslide dams along the drainages in both the zones. One such landslide dam was observed near the village of Mantam close to Mangan along the tributary of the Teesta River during monsoon rains of 2016 (Figure 3b; R. Bhasin et al., 2020; Martha, Roy, & Kumar, 2017; Morken et al., 2020). In addition, this zone also lies to the immediate front of the orographic barrier, and

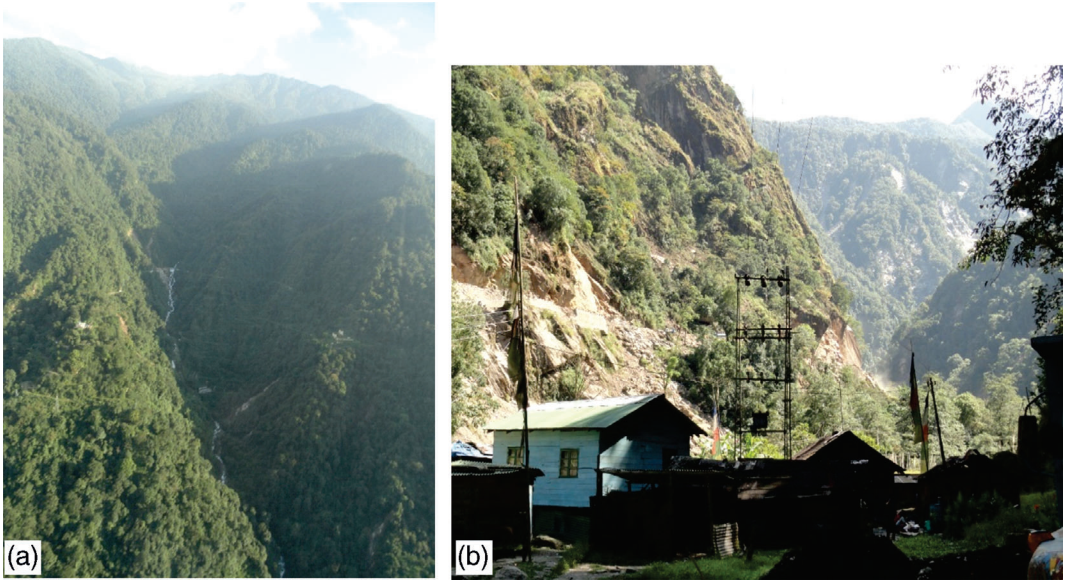

FIGURE 4 View of the slopes in Zone I (a) near Lachung and (b) near Chungthang indicating steep slopes with high relief

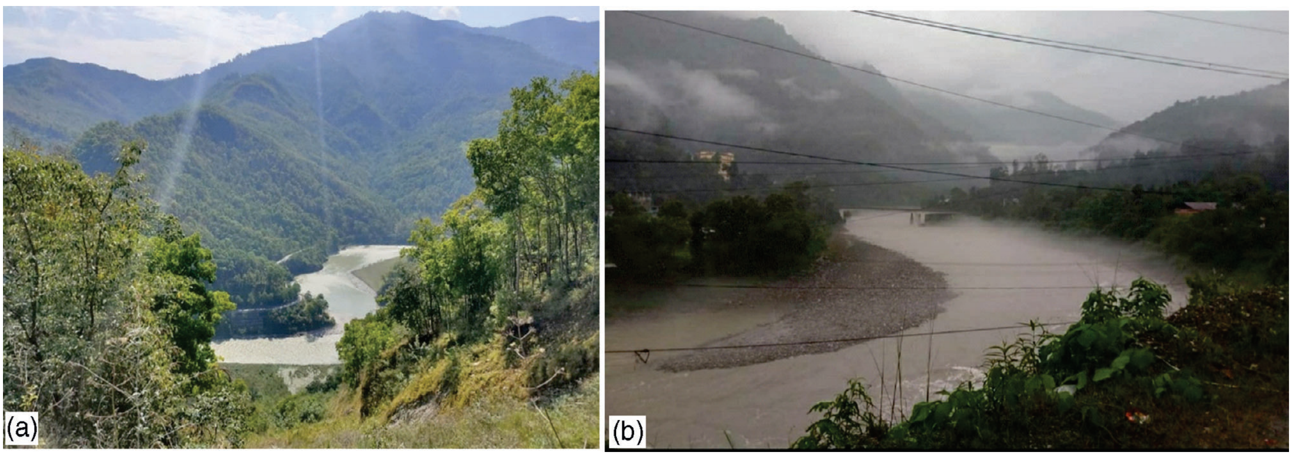

FIGURE 5 The view of the slopes in Zone III indicating (a) gentler slopes and (b) wider valley

thus, higher precipitation is experienced in this zone as compared to rainfall in Zone I (Figure 2). In view of this, it is expected that slopes in the regions are unstable, primarily due to the higher tectonic activity, and these are triggered due to the higher rainfall. Therefore, some of the large deep-seated chronic landslides such as Rangrang landslide (Figure 3a), Lanta Khola landslide (Figure 3c), and Mangan landslide (Figure 3d) are present in this zone. Besides, there are many small-scale landslides in this zone that causes frequent damages in the zone.

Zone III, located in the Lesser Himalaya, is characterized by the lowest steepness index, lower stream length gradient index, and the highest valley floor width to valley height ratio, and thus exhibits the lowest tectonic activity (Bull, 2009; Jamir et al., 2020; Kumar et al., 2019) as compared to the tectonic activity in Zones I and II. This is also evidenced by the gentle channel gradient of Teesta River, gentler valley slopes, and wider valleys (Figure 5a,b) in this part of the area. Thus, the inherent tectonic activity of the region in this part of the valley is not conducive for the development of land sliding. However, other factors like excessive rainfall and the anthropogenic activity dominate the causes of landslides in this zone. The lower activity in this zone is also reflected by relatively lower erosion in this part of the valley (Abrahami, Van Der Beek, Huyghe, Hardwick, & Carcaillet, 2016).

In addition to the inherent tectonic activity, the distribution of rainfall also influences the occurrence of landslides in the area. Starkel (1972) indicated that the topographic relief of the area has been carved and influenced by the catastrophic rainfall. The swath profile indicates that there is abrupt increase in elevation in Zones I and II, and the mountains to the north of the MCT act as the orographic barrier restricting the movement of the moisture laden winds towards the north (Bookhagen & Burbank, 2006). It is for this reason that higher rainfall is experienced towards moving from north to south; however, its intensity greatly increases in Zone II near the

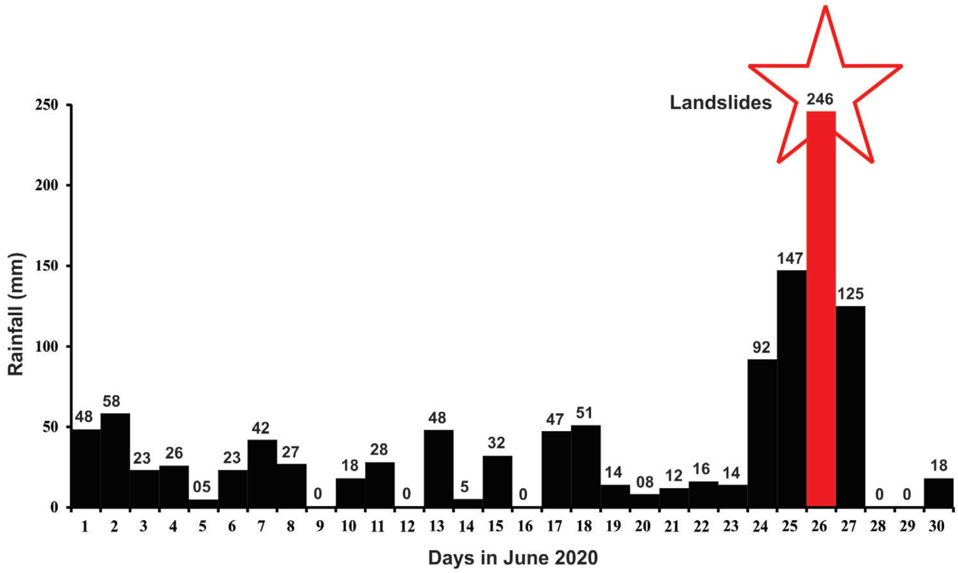

FIGURE 6 Bar diagram of the daily rainfall for the month of June 2020. Note the excessive rainfall for 4 days during 24–27 June 2020, whereas the normal rainfall during June in the area is ~485 mm

FIGURE 7 Debris slide due to excessive rainfall during June 2020 in the vicinity of Mangan township (courtesy: http://savethehills.blogspot.com/)

orographic barrier, or towards the south of it, in the Mangan Chungthang region. It is owing to the higher tectonic activity and the higher amount of precipitation in Zone II, this zone is characterized by some of the major landslides (Figure 3a–d) which are mostly active during the monsoon. It is important to mention here that during June 2020, the area received ~1,160 mm of rainfall, of which ~610 mm fell during 4 days (Figure 6) causing many slopes in the region to fail and also resulting in the damaging of the buildings (Figure 7).

The inherent tectonic activity is one of the dominant causes of landslides in the Higher Himalaya, and the rainfall and anthropogenic activity in the Lesser Himalaya have also been reported from other parts of the Himalaya (Kumar et al. 2019; Jamir et al., 2020). It is further observed that it is the rockfall or the rock avalanche that dominates in the Higher Himalaya and the debris slide or the debris flow in the Lesser Himalaya. The present study also supports the studies carried out by Kumar et al., (2019) and Jamir et al., (2020). However, the present area of studies is seismically very active, and has experienced numerous earthquakes in the past. The inventory of landslides prepared after the 2011 Sikkim earthquake indicates that most of landslides are located in the area where the tectonic activity is pronounced, that is, in Zone I and Zone II (Gupta et al., 2015; Mahajan et al., 2012; Martha et al., 2015).

6 | CONCLUSIONS

From this study, the following conclusions can be drawn:

- In the Higher Himalaya, particularly in Zone I, the landslides owe their origin mainly to the higher tectonic activity. The rainfall in this zone has least effect on the distribution of landslides, as the area is located behind the orographic barrier.
- The landslides in Zone II, that is, between Chungthang and Rangrang, are dominantly controlled by the tectonic activity, and are also influenced by higher rainfall, particularly between Mangan and Rangrang, as this area lies to the front of the orographic barrier.

- Some of the bigger landslides in the vicinity of Mangan owe their origin to the tectonic activity of the area and are triggered by high rainfall.
- Landslides in the Lesser Himalaya in Zone III, that is, between Rangrang and Rangpo, dominantly owe their origin to rainfall and not to the tectonic activities. Therefore, this zone accounts for the presence of the debris landslide.

Since there are many studies depicting higher tectonic activity in many parts of the Himalaya, the present study will be useful to demarcate areas having higher propensity towards landslides, particularly in the present climate change scenario where concentrated rainfall are common in the Himalayan terrain.

ACKNOWLEDGEMENTS

The present work is an outcome of the jointIndo-Norwegian bilateral program, funded by the Ministry of Earth Sciences(MoES) (MoES/Indo-Nor/PS-2/2015)), New Delhi, India and the Research Council ofNorway (NFRno. 248774), Norway. The funding for this work to the Wadia Institute of Himalayan Geology, Dehradun (India), Indian Institute of Technology, Kharagpur (India), GeologicalSurvey of Norway, Trondheim (Norway), and Norwegian Geotechnical Institute, Oslo (Norway) is thankfully acknowledged.

CONFLICT OF INTEREST

The authors declare no conflicts of interest.

DATA AVAILABILITY STATEMENT

The data that support the findings of this study are available on request from the corresponding author. The data are not publicly available due to privacy or ethical restrictions.

ORCID

Vikram Gupta https://orcid.org/0000-0002-9147-365X
John Dehls https://orcid.org/0000-0002-8054-3544

REFERENCES

Abrahami, R., Van Der Beek, P., Huyghe, P., Hardwick, E., & Carcaillet, J. (2016). Decoupling of long-term exhumation and short-term erosion rates in the Sikkim Himalaya. *Earth and Planetary Science Letters*, *433*, 76–88.

Acharyya, S. K. (1980). Geochemistry and geotectonic implication of basic volcanic rocks in the Lower Gondwana sequence (Upper Palaeozoic) of the Sikkim Himalayas. *Geological Magazine*, *117*(6), 621–629.

Agliardi, F., Crosta, G. B., Frattini, P., & Malusà, M. G. (2013). Giant non-catastrophic landslides and the long-term exhumation of the European Alps. *Earth and Planetary Science Letters*, *365*, 263–274.

Allen, S. K., Cox, S. C., & Owens, I. F. (2011). Rock avalanches and other landslides in the central southern Alps of New Zealand: A regional study considering possible climate change impacts. *Landslides*, *8*(1), 33–48.

Anbalagan, R., Kumar, R., Lakshmanan, K., Parida, S., & Neethu, S. (2015). Landslide hazard zonation mapping using frequency ratio and fuzzy logic approach, a case study of Lachung valley, Sikkim. *Geoenvironmental Disasters*, *2*(6), 1–17.

Anbarasu, K., Sengupta, A., Gupta, S., & Sharma, S. P. (2010). Mechanism of activation of the Lanta Khola landslide in Sikkim Himalayas. *Landslides*, *7*, 135–147.

Bhasin, R., Shabanimashcool, M., Hermanns, R. L., Morken, O. A., Dehls, J. F., Gupta, V., & Sengupta, A. (2020). Back analysis of shear strength parameters of a large rock slide in Sikkim Himalaya. *Journal of Rock Mechanics and Tunnelling Technology*, *26*(2), 81–92.

Bhasin, R. K., Grimstad, E., Larsen, J. O., Dhawan, A. K., Singh, R., Verma, S. K., & Venkatachalam, K. (2002). Landslide Hazards and mitigation measures at Gangtok, Sikkim Himalaya. *Engineering Geology*, *64*, 351–368.

BIS Code 1893. (2002). *Earthquake hazard zoning map of India*. Retrieved from www.bis.org.in

BMTPC. (2003). *Landslide hazard zonation atlas of India*. Building Materials and Technology Promotion Council, Government of India and Anna University, Chennai, p. 125.

Bookhagen, B., & Burbank, D. W. (2006). Topography, relief and TRMM-derived rainfall variations along the Himalaya. *Geophysical Research Letters*, *33*, L08405.

Bull, W. B. (2009). *Tectonically active landscapes* (p. 326). Oxford, England: Wiley-Blackwell.

Bull, W. B., & McFadden, L. D. (1977, 1977). Tectonic geomorphology north and south of the Garlock Fault, California. In D. O. Doehering (Ed.), *Geomorphology in arid regions, Proceedings at the Eighth Annual Geomorphology Symposium* (pp. 115–138). Binghamton, NY: State University of New York.

Dortch, J. M., Owen, L. A., Haneberg, W. C., Caffee, M. W., Dietsch, C., & Kamp, U. (2009). Nature and timing of large landslides in the Himalaya and Trans Himalaya of northern India. *Quaternary Science Reviews*, *28*(11–12), 1037–1054.

Froude, M. J., & Petley, D. N. (2018). Global fatal landslide occurrence from 2004 to 2016. *Natural Hazards and Earth System Sciences*, *18*(8), 2161–2181.

Gerrard, J. (1994). The landslide hazard in the Himalayas: Geological control and human action. In M. Morisawa (Ed.), *Geomorphology and natural hazards* (pp. 221–230). Binghamton, NY: Elsevier.

Ghosh, S., & Carranza, E. J. M. (2010). Spatial analysis of mutual fault/fracture and slope controls on rocksliding in Darjeeling Himalaya, India. *Geomorphology*, *122*(1–2), 1–24.

Gupta, V., Mahajan, A. K., & Thakur, V. C. (2015). A study on landslides triggered during Sikkim Earthquake of September 18, 2011. *Himalayan Geology*, *36*(1), 81–90.

Gupta, V., Tandon, R. S., Venkateshwarlu, B., Bhasin, R. K., & Kaynia, A. M. (2017). Accelerated mass movement activities due to increased rainfall in the Nainital township, Kumaun Lesser Himalaya, India. *Zeitschrift für Geomorphologie*, *61*(1), 29–42.

Hack, J. T. (1973). Stream-profile analysis and stream-gradient index. *Journal of Research of the US Geological Survey*, *1*(4), 421–429.

Hermanns, R. L., Niedermann, S., Garcia, A. V., Gomez, J. S., & Strecker, M. R. (2001). Neotectonics and catastrophic failure of mountain fronts in the southern intra-Andean Puna Plateau, Argentina. *Geology*, *29*(7), 619–622.

Hewitt, K. (1988). Catastrophic landslide deposits in the Karakoram Himalaya. *Science*, *242*(4875), 64–67.

Hewitt, K. (2002). Postglacial landform and sediment associations in a landslide-fragmented river system: The Trans Himalayan Indus streams, central Asia. In *Landscapes of transition* (pp. 63–91). Dordrecht, The Netherlands: Springer.

Hewitt, K. (2006). Disturbance regime landscapes: Mountain drainage systems interrupted by large rockslides. *Progress in Physical Geography*, *30*(3), 365–393.

Hovius, N., Stark, C. P., & Allen, P. A. (1997). Sediment flux from a mountain belt derived by landslide mapping. *Geology*, *25*(3), 231–234.

Jamir, I., Gupta, V., Thong, G. T., & Kumar, V. (2020). Litho-tectonic and precipitation implications on landslides, Yamuna valley, NW Himalaya. *Physical Geography*, *41*(4), 365–388.

Keller, E. A., & Pinter, N. (1996). *Active tectonics* (p. 359). Upper Saddle River, NJ: Prentice Hall.

Korup, O., Densmore, A. L., & Schlunegger, F. (2010). The role of landslides in mountain range evolution. *Geomorphology*, *120*(1–2), 77–90.

Krautblatter, M., Funk, D., & Günzel, F. K. (2013). Why permafrost rocks become unstable: A rock–ice-mechanical model in time and space. *Earth Surface Processes and Landforms*, *38*(8), 876–887.

Kumar, V., Gupta, V., & Sundriyal, Y. P. (2019). Spatial interrelationship of landslides, litho-tectonic, and climate regime, Satluj valley, Northwest Himalaya. *Geological Journal*, *54*(1), 537–551.

Larsen, I. J., & Montgomery, D. R. (2012). Landslide erosion coupled to tectonics and river incision. *Nature Geoscience*, *5*(7), 468–473.

Li, G. K., & Moon, S. (2021). Topographic stress control on bedrock landslide size. *Nature Geoscience*, *14*, 307–313.

Mahajan, A. K., Gupta, V., & Thakur, V. C. (2012). Macroseismic field observations of 18 September 2011 Sikkim earthquake. *Natural Hazards*, *63*(2), 589–603.

Martha, T. R., Govindharaj, K. B., & Kumar, K. V. (2015). Damage and geological assessment of the 18 September 2011 Mw 6.9 earthquake in Sikkim, India using very high resolution satellite data. *Geoscience Frontiers*, *6*(6), 793–805.

Martha, T. R., Roy, P., & Kumar, K. V. (2017). Assessment of the valley-blocking 'So Bhir' landslide near Mantam village, North Sikkim, India, using satellite images. *Current Science*, *113*(7), 1228–1229.

Mehrotra, G. S., Sarkar, S., Kanungo, D. P., & Mahadevaiah, K. (1996). Terrain analysis and spatial assessment of landslide hazards in parts of Sikkim Himalaya. *Journal Geological Society of India*, *47*, 491–498.

MHA, Government of India. (2011). *Disaster management in India*. New Delhi, India: Ministry of Home Affairs, Government of India.

Morken, O. A., Hermanns, R. L., Penna, I., Dehls, J. F., & Bhasin, R. (2020). *The Dzongu landslide dam: High sedimentation rate contributing to dam stability*, *ISRM International Symposium—EUROCK 2020*, International Society for Rock Mechanics and Rock Engineering, p. 8.

Nadim, F., Kjekstad, O., Peduzzi, P., Herold, C., & Jaedicke, C. (2006). Global landslide and avalanche hotspots. *Landslides*, *3*(2), 159–174.

Panthi, K. K., & Nilsen, B. (2006). Numerical analysis of stresses and displacements for the Tafjord slide, Norway. *Bulletin of Engineering Geology and the Environment*, *65*, 57–63.

Penna, I., Hermanns, R., Nicolet, P., Morken, O. A., Dehls, J., Gupta, V., & Jaboyedoff, M. (2021). Airblasts caused by large slope collapses. *GSA Bulletin*, *133*(5–6), 939–948.

Penna, I. M., Hermanns, R. L., Niedermann, S., & Folguera, A. (2011). Multiple slope failures associated with neotectonic activity in the southern Central Andes (37°–37° 30′ S), Patagonia, Argentina. *Geological Society of America Bulletin*, *123*(9–10), 1880–1895.

Petley, D. (2012). Global patterns of loss of life from landslides. *Geology*, *40*(10), 927–930.

Petley, D. N., Hearn, G. J., Hart, A., Rosser, N. J., Dunning, S. A., Oven, K., & Mitchell, W. A. (2007). Trends in landslide occurrence in Nepal. *Natural Hazards*, *43*(1), 23–44.

Saha, D. (2013). Lesser Himalayan sequences in Eastern Himalaya and their deformation: Implications for Paleoproterozoic tectonic activity along the northern margin of India. *Geoscience Frontiers*, *4*(3), 289–304.

Sanchez, G., Rolland, Y., CorsinI, M., Braucher, R., Bourlès, D., Arnold, M., & Aumaître, G. (2010). Relationships between tectonics, slope instability and climate change: Cosmic ray exposure dating of active faults, landslides and glacial surfaces in the SW Alps. *Geomorphology*, *117*(1–2), 1–13.

Sengupta, A., Gupta, S., & Anbarasu, K. (2010). Rainfall thresholds for the initiation of landslide at Lanta Khola in north Sikkim, India. *Natural Hazards*, *52*(1), 31–42.

Sharma, S. P., Anbarasu, K., Gupta, S., & Sengupta, A. (2010). Integrated very low-frequency EM, electrical resistivity, and geological studies on the Lanta Khola landslide, North Sikkim, India. *Landslides*, *7*(1), 43–53.

Shroder, J. F., & Bishop, M. P. (1998). Mass movement in the Himalaya: New insights and research directions. *Geomorphology*, *26*(1–3), 13–35.

Singh, K. K., & Singh, A. (2016). Detection of 2011 Sikkim earthquake-induced landslides using neuro-fuzzy classifier and digital elevation model. *Natural Hazards*, *83*(2), 1027–1044.

Starkel, L. (1972). The role of catastrophic rainfall in the shaping of the relief of the lower Himalaya (Darjeeling Hills). *Geographia Polonica*, *21*, 103–147.

Tandon, R. S., Gupta, V., & Venkateshwarlu, B. (2021). Geological, Geotechnical, and GPR investigations along the Mansa Devi hill-bypass (MDHB) Road, Uttarakhand, India. *Landslides*, *18*, 849–863. https://doi.org/10.1007/s10346-020-01546-9.

Trauth, M. H., Alonso, R. A., Haselton, K. R., Hermanns, R. L., & Strecker, M. R. (2000). Climate change and mass movements in the NW Argentine Andes. *Earth and Planetary Science Letters*, *179*(2), 243–256.

Weidinger, J. T., & Korup, O. (2009). Frictionite as evidence for a large Late Quaternary rockslide near Kanchenjunga, Sikkim Himalayas, India—Implications for extreme events in mountain relief destruction. *Geomorphology*, *103*(1), 57–65.

Wobus, C. W., Whipple, K. S., Kirby, E., Snyder, N. P., Johnson, J., Spyropolou, K., … Sheehan, D. (2006). Tectonics from topography: Procedures, promise, and pitfalls. In S. D. Willett, N. Hovius, M. T. Brandon, & D. M. Fisher (Eds.), *Tectonics, climate and landscape evolution*. Geological Society of America Special Paper 398, Penrose Conference Series (pp. 55–74). Boulder, CO: Geological Society of America.

How to cite this article: Gupta, V., Chauhan, N., Penna, I., Hermanns, R., Dehls, J., Sengupta, A., & Bhasin, R. K. (2022). Geomorphic evaluation of landslides along the Teesta river valley, Sikkim Himalaya, India. *Geological Journal*, 1–11. https://doi.org/10.1002/gj.4377